

# 965. Automatic artifacts removal from epileptic EEG using a hybrid algorithm

Jing Wang<sup>1</sup>, Qing Zhang<sup>2</sup>, Yizhuo Zhang<sup>3</sup>, Guanghua Xu<sup>4</sup>

School of Mechanical Engineering, Xi'an Jiaotong University, Xi'an 710049, China

<sup>2</sup>Corresponding author

E-mail: <sup>1</sup>wangpele@gmail.com, <sup>2</sup>zhangq@mail.xjtu.edu.cn, <sup>3</sup>aii@mail.xjtu.edu.cn,

<sup>4</sup>xugh@mail.xjtu.edu.cn

(Received 31 January 2013; accepted 28 February 2013)

**Abstract.** Electroencephalogram (EEG) examination plays a very important role in the diagnosis of disorders related to epilepsy in clinic. However, epileptic EEG is often contaminated with lots of artifacts such as electrocardiogram (ECG), electromyogram (EMG) and electrooculogram (EOG). These artifacts confuse EEG interpretation, while rejecting EEG segments containing artifacts probably results in a substantial data loss and it is very time-consuming. The purpose of this study is to develop a novel algorithm for removing artifacts from epileptic EEG automatically. The collected multi-channel EEG data are decomposed into statistically independent components with Independent Component Analysis (ICA). Then temporal and spectral features of each independent component, including Hurst exponent, skewness, kurtosis, largest Lyapunov exponent and frequency-band energy extracted with wavelet packet decomposition, are calculated to quantify the characteristics of different artifact components. These features are imported into trained support vector machine to determine whether the independent components represent EEG activity or artifactual signals. Finally artifact-free EEGs are obtained by reconstructing the signal with artifact-free components. The method is evaluated with EEG recordings acquired from 15 epilepsy patients. Compared with previous work, the proposed method can remove artifacts such as baseline drift, ECG, EMG, EOG, and power frequency interference automatically and efficiently, while retaining important features for epilepsy diagnosis such as interictal spikes and ictal segments.

**Keywords:** epilepsy, electroencephalogram (EEG), automatic artifacts removal, independent component analysis (ICA), support vector machine (SVM), wavelet packet decomposition.

## 1. Introduction

Epilepsy is one of the most common neurological disorders and affects almost 60 million people worldwide. In clinic, the presence of epileptiform events in the epileptic EEGs, such as interictal spikes and sharps, spike and slow rhythm, confirms the diagnosis of epilepsy or localizes the epileptic areas [1]. Standard EEG recordings often contain some large and distracting artifacts, such as muscle noise (EMG), eye movement and blink (EOG), cardiac signals (ECG) and line noise, etc. The existence of these artifacts leads to serious problem for the interpretation and analysis of EEGs [2]. Rejecting EEG segments with artifacts larger than a preset threshold is a commonly used method for dealing with artifacts. However the data loss to artifact rejection may be unacceptable in case that epileptic events and artifacts occur at approximately the same time [3]. In the past decades artifact removal has been a fundamental issue in EEG processing and many researchers are involved in it.

Majority of previous attempts are mainly focused on the removal of ocular artifacts. Typical methods are based on independent component analysis (ICA) [4-9]. It can separate the observed EEG into statistically independent sources including ECG, EOG, EMG and EEG, etc. One major problem of ICA is the necessity to manually identify each component as artifactual or not. As a result, artifact removal methods based on single ICA are semiautomatic. Several attempts have been made to develop new methods which can eliminate artifacts automatically [4-7]. Boudet proposed methods that identify ICA sources by comparing variance between rest instant and artifact instant [5]. The main drawback of the methods is that they require a learning step to get

the distribution of artifactual activity.

In this paper we present a new method that can automatically remove a wide variety of artifacts in epileptic EEG based on ICA and support vector machine. The content of this study is laid out in 4 sections with this section as the introduction. In section 2, the detailed algorithm for automatic artifact removal is explored. The acquired EEG signals are first decomposed into statistically independent components using ICA. Each independent component is then partitioned into 5 s epochs. Eight quantitative features are extracted to describe the characteristics of different artifact components. The extracted features are input into support vector machine to identify the artifact components and the EEG data is reconstructed by eliminating the artifact components. The validity of the method is evaluated with clinical epileptic EEG in section 3. Finally, discussion and conclusion are given in section 4.

## 2. Materials and methods

### 2.1. Data set

Scalp EEG recordings were collected from Zhejiang Provincial People's Hospital, China. The patients (12 females and 19 males, age:  $32.8 \pm 7.7$ ) acquired EEG inspection for diagnosis of epilepsy. Data acquisition system is Phoenix Unique Ambulatory EEG of EMS Handelsges.mbh Company, Austria. EEG signals are amplified with bandpass filter of 0.15–60 Hz and the sampling rate is set to 256 Hz. Exploring cup electrodes were fixed to the scalp at Fp1, Fp2, F3, F4, C3, C4, P3, P4, O1, O2, F7, F8, T3, T4, T5 and T6 according to the International 10–20 System, and the reference electrodes are located on the ipsilateral ear electrodes. Video recordings are acquired synchronously with EEG, by which artifacts such as EOG (e.g. eye blinks) and EMG (e.g. chewing) can be identified. All the subjects give informed consent.

### 2.2. Methods

The fundamental procedure of artifact removal in EEG using ICA-based algorithm consists of three steps: (1) decompose the raw EEG into statistically independent components; (2) identify the artifact components; (3) eliminate the artifact components and reconstruct the signal with the remaining components. The key problem in automatic removal of artifacts is to identify the artifact components automatically. Here statistical features of the components in time and frequency domain are extracted and input into support vector machine to achieve the goal. The flow chart of automatic artifacts removal algorithm is shown in Fig. 1.

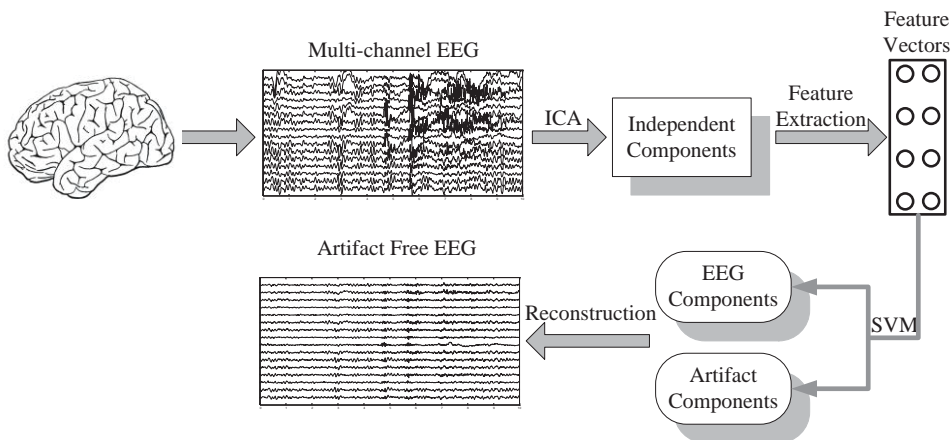


Fig. 1. Block diagram of automatic artifacts removal with ICA and support vector machine

### 2.2.1. ICA

ICA [10] is a signal processing technique which aims at expressing a set of random variables as linear combinations of statistically component variables. It was originally proposed by Comon [11] to solve the BSS problem. The architecture of the problem is illustrated in Fig. 2, where  $\mathbf{S}$  is the unknown source signal and  $\mathbf{Y}$  is the observed signal collected with  $N$  sensors.  $\mathbf{X}$  is the approximation of the unknown sources acquired with the de-mixing matrix  $\mathbf{W}$  and the observed signal  $\mathbf{Y}$ .

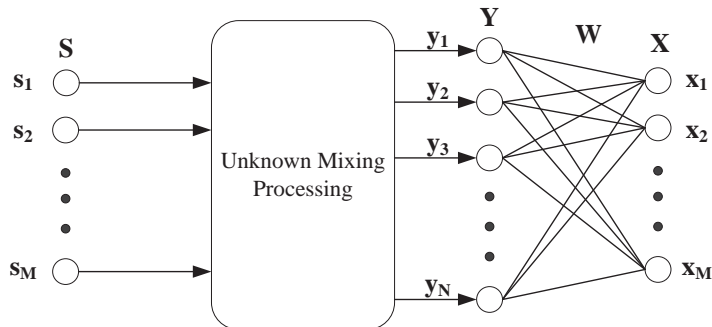


Fig. 2. Architecture of BSS problem

In this paper we apply FastICA algorithm [12] to decompose the acquired EEG data into statistically independent components, using EEGLAB platform [13] running on MATLAB (The Mathworks, Natick, Massachusetts). It works on a non-overlapping window with length of 30 s, which contains sufficient samples to reliably separate the artifact from real EEG activities [8, 14]. The number of extracted independent components is equal to the number of recording electrodes [8]. Some independent components are probably a mixture of EEG and artifactual activities and extracting the features using the entire component may obscure the artifact segments. Thus we partition each 30 s component into six 5 s epochs.

### 2.2.2. Feature extraction

With ICA, artifacts and EEGs are separated into different independent components. Traditionally the identification of artifact components is achieved manually by observing the scalp maps and the fuzzy characteristics (in time and frequency domain) of the components. In order to identify the artifact segments automatically, we need to define quantitative features that can discriminate the artifact components from the EEG components. Here features in time and frequency domain, including Hurst exponent, skewness, Kurtosis, largest Lyapunov exponent and frequency-band energy, are selected.

**Hurst exponent.** Hurst exponent was first proposed by Hurst in 1965 [15]. It is used to evaluate the long-range dependence of a time series. Hurst exponent is usually calculated by the recurrent method [9] and ranges from 0 to 1.  $H = 0.5$  corresponds to a standard Brownian movement, and  $0 < H < 0.5$  indicates the anti-persistent behavior, while  $0.5 < H < 1$  describes a temporally persistent or trend reinforcing time series. Obviously linear electrode artifact (e.g. baseline drift) has higher Hurst exponent than that of EEGs because of longer persistence. Furthermore extensive computer experiments show that artifacts such as eye blinking and heart beats have lower Hurst exponent than that of EEGs [9].

**Skewness.** Skewness corresponds to the third-order statistic of the data. An EEG recording that contains eye blink or baseline drift typically has a positive or negative skewness since the eye blinking artifact or the baseline drift artifact increases locally the asymmetry of the signal [16]. Here we take the absolute value of the skewness. As a result, the eye blink and baseline

drift have larger skewness than that of normal EEGs, which are approximately symmetrically distributed.

**Kurtosis.** Kurtosis is the 4th cumulant of a time series, which quantifies how outlier-prone a distribution is [4]. Highly positive kurtosis indicates that the distribution of the signal is peak and sparse, and the identified activity is probably to be an artifact such as eye movements or ECG. The kurtosis of the normal distribution is 3, while the kurtosis of a periodical series is negative and the kurtosis of Gaussian noise is close to 0.

**Largest Lyapunov exponent.** Lyapunov exponent is a quantitative measure of the sensitive dependence on the initial conditions, which defines the average exponential rate of the divergence or convergence of the nearby orbits in the phase space. Specifically LLE is very useful in recognizing some basic rhythms that exist periodically in normal EEGs, as well as rhythmic seizure onsets in epileptic EEGs. When calculating LLE of EEG signals, an embedding dimension between 5 to 20 and a delay of 1 are proper [17]. In this paper we set the embedding dimension to 10 and delay to 1.

**Frequency-band energy.** Besides the above mentioned features in time domain, features in frequency domain are also useful, i.e. some of the artifacts have unique frequencies. Here we employ sub-band energy based on wavelet packet decomposition as features in frequency domain.

First each epoch is filtered between 0.3 and 60 Hz with a 10th order digital Butterworth. Then Wavelet Packet Decomposition (WPD) is applied to split the epoch into two orthonormal subspaces  $V$  and  $W$ , where  $V$  and  $W$  include low and high frequency information of the original epoch, respectively. With multi-level decomposition, WPD leads to a complete wavelet packet tree, shown in Fig. 3. Thereinto,  $U_{j,n}$  is the  $n$ th ( $n$  is the frequency factor,  $n = 0, 1, 2, \dots, 2^j - 1$ ) subspace of wavelet packet at  $j$ th scale, and  $U_{j,k}^n(t) = 2^{-j/2}u^n(2^{-j}t - k)$  indicates the corresponding orthonormal basis ( $k$  is the shift factor), which satisfies with:

$$u_{j,0}^n(t) = \begin{cases} \sum_k h_0(k)u_{j-1,k}^i & \text{if } n \text{ is even,} \\ \sum_k h_1(k)u_{j-1,k}^i & \text{if } n \text{ is odd,} \end{cases} \quad (1)$$

where  $j, k \in Z, n = 0, 1, 2, \dots, 2^j - 1$ ,  $h_0(k)$  and  $h_1(k)$  are a couple of quadruple mirror filters (QMF) which are irrelevant to scales and satisfy with:

$$h_1(k) = (-1)_{1-k}h_0(1 - k). \quad (2)$$

The coefficient of WPD at  $j$ th level and  $k$ th sample can be calculated with:

$$d_j^m(k) = \begin{cases} \sum_m h_0(m - 2k)d_{j-1}^{n/2}(m) & \text{if } n \text{ is even,} \\ \sum_m h_1(m - 2k)d_{j-1}^{(n-1)/2}(m) & \text{if } n \text{ is odd.} \end{cases} \quad (3)$$

When we decompose the signal to  $j$ th level, the frequency ranges of all the subspaces are  $\{[0, f_s/2^{j+1}], [f_s/2^{j+1}, 2f_s/2^{j+1}], [2f_s/2^{j+1}, 3f_s/2^{j+1}], \dots, [(2j - 1)f_s/2^{j+1}, f_s/2]\}$ , where  $f_s$  is the sampling frequency. For a selected sub-band, its energy can be obtained by:

$$E_{j,n} = \sum_k (d_j^n(k))^2. \quad (4)$$

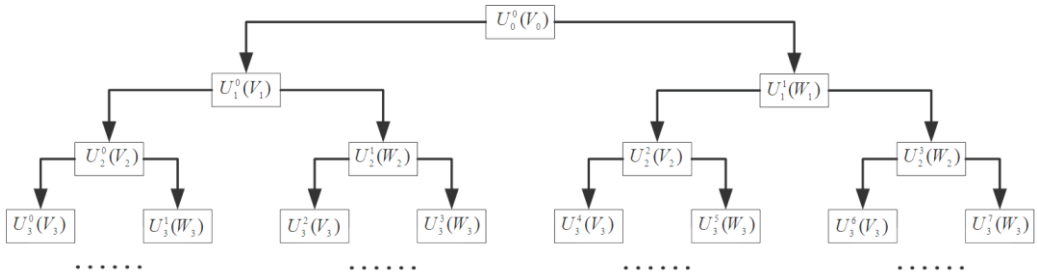


**Fig. 3.** Wavelet packet decomposition tree

Previous researchers show that significant power at low frequencies might suggest the presence of ocular or movement artifacts, while the power in the high-frequency band would indicate EMG contamination [8]. Furthermore some basic rhythms in EEG have specific frequency ranges and can be identified with frequency-band energy. In this paper we select Daubechies Wavelet (db4) [18-19] to decompose each 5 s epoch to 4-level wavelet packet and calculate the sub-band energy of 0~3.75 Hz, 3.75~15 Hz, 15~30 Hz, 30~60 Hz, namely,  $\{E_{4,0}, E_{4,1} + E_{3,1}, E_{2,1}, E_{1,1}\}$  as the features in the frequency domain.

### 2.2.3. Classification using support vector machine

Support vector machine is an efficient tool for solving supervised classification problems due to its generalization performance and established empirical performance. The basic idea of classification with SVM is to project the sample space into a high-dimensional eigenspace and find an optimal separating hyperplane (OSH) for a given feature set, which maximizes the margin between the training data and the decision boundary. The subsets of the patterns that are closest to the decision boundary are called support vectors. The construction of OSH can be posted as the following quadratic optimization problem:

$$\min_{\mathbf{w}} \frac{1}{2} (\mathbf{w}^T \mathbf{w}) \quad \text{s. t. } d^s ((\mathbf{w}^T \mathbf{x}^s) + b) \geq 1, \quad (5)$$

where  $d^s \in \{-1, 1\}$  represents the  $s$ th desired output,  $\mathbf{x}^s \in R^p$  is the  $s$ th input sample of the training data set  $\{\mathbf{x}^s, d^s\}_{s=1}^S$  containing eight features:  $\mathbf{x}^s = [HE^s, SK_k^s, KU^s, LLE^s, E_{4,0}^s, (E_{4,1} + E_{3,1})^s, E_{2,1}^s, E_{1,1}^s]$ , and  $S$  is the number of training vectors.  $HE$ ,  $SK$  and  $KU$  stand for Hurst exponent, skewness and kurtosis, respectively. In practice the OSH probably does not exist. Hence the slack parameters  $\xi_s \geq 0, s = 1, 2, \dots, S$  are introduced. The optimization problem now becomes:

$$\min_{\mathbf{w}, \xi} \frac{1}{2} (\mathbf{w}^T \mathbf{w}) + C \sum_{s=1}^S \xi_s \quad (6)$$

s. t.  $d^s ((\mathbf{w}^T \mathbf{x}^s) + b) \geq 1 - \xi_s; \xi_s \geq 0, s = 1, 2, \dots, S,$

where  $C$  stands for the misclassification penalty term and can be considered as the regularization parameter. A larger  $C$  indicates higher penalty to the training errors. By introducing Lagrange multipliers  $\alpha_s$ , the OSH is computed as a decision surface:

$$f(\mathbf{x}) = \text{sgn} \left( \sum_{s=1}^S d^s \alpha_s K(\mathbf{x}, \mathbf{x}^s) + b \right), \quad (7)$$

where  $\text{sgn}(\cdot) \in \{\pm 1\}$ ,  $\mathbf{x}$  are support vectors and  $K(\cdot)$  is the kernel function. A kernel for a nonlinear support vector machine projects the samples to a feature space of higher dimension via a nonlinear mapping function. Here we employ the radial-based function (RBF) defined as:

$$K(\mathbf{x}, \mathbf{x}^s) = \exp(-\|\mathbf{x} - \mathbf{x}^s\|/2\sigma^2), \quad (8)$$

where  $\sigma$  is the adjustable parameter that governs the variance of the kernel function.

### 3. Results

16 patients are selected to train the algorithm, while the remaining 15 patients are used as validation set. Each patient has 10 min recordings with 16 electrodes.

#### 3.1. Training the algorithm

The acquired EEG signals are first decomposed into independent components using ICA. Each independent component is partitioned into six 5 s epochs. Features including Hurst exponent, skewness, kurtosis, largest Lyapunov exponent and frequency-band energy, are then calculated and input into support vector machine for classification. Altogether we have  $16 \times 16 \times 10 \times 2 = 5120$  independent components (or  $16 \times 16 \times 10 \times 2 \times 6 = 30720$  5 s epochs) to train the support vector machine. 15360 epochs are selected as training set while others are test set. In the training set there are 6324 epochs containing different types of artifacts and 9036 free of artifact. The artifact epochs include 72 power frequency interference, 1266 EOG, 4481 EMG, 116 ECG and 389 baseline drift. In the test set 5100 epochs containing artifacts and 10260 free of artifacts are involved. The artifact epochs contain 31 power frequency interference, 932 EOG, 3938 EMG, 60 ECG and 139 baseline drift.

The average error of the support vector machine is estimated as follows. Firstly 1280 independent components (7680 epochs) of the training set are randomly selected as training samples and 1280 independent components (7680 epochs) of the test set are randomly decided as test samples. Two experienced clinicians are asked to review all the independent components to decide whether it is artifact or not. Feature vectors of the training samples are then calculated to train the support vector machine and the support vectors of the support vector machine are obtained. After that feature vectors of the test samples are calculated and input into the trained support vector machine for classification. The sum of epochs representing artifacts is then used to determine whether to reject or preserve each independent component. A threshold  $T_h$  is chosen to get minimum classification error. If the threshold is too high, some artifacts are probably preserved. If the threshold goes too low, lots of normal EEGs will be lost [8]. Besides the threshold, two important parameters in support vector machine,  $C$  and  $\sigma$ , have a decisive effect on the classification accuracy [16]. In order to find the optimal  $T_h$ ,  $C$  and  $\sigma$ , we calculate the average of classification error with a predefined range of these parameters. The above process is performed ten times to yield average of the classification error. The optimal  $T_h$ ,  $C$  and  $\sigma$ , which correspond to the lowest classification error, are found to be 4, 500 and 7, respectively. With the optimized parameters we obtain an average training error of 4.91 % and the average number of support vectors is 13.2 % of the training data set size.

#### 3.2. Testing the algorithm

We apply the algorithm with optimal parameters to the validation set (15 patients). After ICA we obtain  $15 \times 16 \times 10 \times 2 = 4800$  independent components with duration of 30 s. First a typical performance of the proposed method on normal EEG is shown in Figure 4. Since 30 s window is too compressed to depict low-frequency information of the EEG data as well as the independent components, we only draw 1/3 in length, i.e. 10 s. In Fig. 4(a) 10 s EEG is contaminated by

artifacts in numerous channels. Four eye blinks occur at 0.5 s, 2.8 s, 6.2 s and 8 s on Fp1 and Fp2, respectively (see the square boxes). Besides obvious EMG artifacts can be found at 4.8 s on F8, 5.6 s on F7 and T3, 4.8 s and 5.6 s on T4, respectively (see the ellipses). P3, P4, O1 and O2 are also slightly contaminated by EMG artifacts. Fig. 4(b) shows the decomposed independent components. We can find eye blink features on IC1, which is also demonstrated in the scalp map. Obvious EMG artifacts exist on IC2, IC3, IC5, IC7, IC11, IC12 and IC13. For example, scalp maps show that IC2 includes movement artifact on the left hemisphere, while IC13 indicates chewing artifact on the right. Besides IC8, IC15 and IC16 are also identified as artifact components by our algorithm. The signals are reconstructed with the remaining independent components, i.e. IC4, IC6, IC9, IC10 and IC14, shown in Fig. 4(c). We can still find very few chewing artifacts at 4.8 s and 5.6 s on F8, T3, T4 and T6. Previous studies also show that it is rather difficult to remove chewing artifacts completely since they spread in numerous channels with large amplitude. Note the scale difference between Fig. 4(a), (b) and (c).

Next we apply the proposed method to ictal EEG, shown in Fig. 5. Ictal events on O1 and O2 (see the big square box) shown in Fig. 5(a) and simultaneous video recordings confirm an occipital seizure. Epileptic spike waves are also presented at 28.5 s on Fp1 and F8 (see the small square boxes). EMG artifacts exist on T4 throughout the 10 s window (see the ellipse). The decomposed independent components are shown in Fig. 5(b). IC13 is composed of muscle artifacts. With the scalp map it can be concluded as movement artifacts on the right hemisphere. In addition, with the scalp map as well as the waveform of IC1, we believe IC1 is a rhythmic activity on occipital area, which is also to be confirmed by calculating the *LLE* of IC1 (-0.2235). Reconstructed EEGs are shown in Fig. 5(c). EMG artifacts on T4 are removed completely, while ictal events on O1 and O2 are fully retained. Meanwhile epileptic spike waves on Fp1 and F8 are preserved and a spike wave on T5 which is not marked in Fig. 5(a) is also detected.

The performance of the algorithm on the validation set is shown in Table 1 and the results are justified by two clinicians at Zhejiang Provincial People's Hospital. The global average classification error is 10.54 %. As stated before, in the training process, the training and testing samples are randomly selected from 16 patients. Though the two samples are non-overlapping, part of them are probably from the same patients, which indicates that they have similar characteristics. However, in the validation process, the validation set is from other 15 patients and independent from the training and testing samples. This is why the average testing error (10.54 %) is much higher than the average training error (4.91 %). Even so, it shows that the proposed method has promising generalization ability.

Besides the global classification error, we also measure the classification error of epileptic EEG components, which indicates the number of epileptic components that are removed. Thereinto, no epileptic components are removed in 3 out of 15 patients (patient #1, #9, #10). In patient #3, 10 out of 87 epileptic components are classified as artifacts. We explored the EEG recordings and found that these epileptic components are severely contaminated by heavy muscle artifacts during epileptic seizures. Further we scanned all the misclassified epileptic components for the remaining 11 patients and obtained similar results. Relatively, nearly all the epileptic components during interictal period are correctly classified. In general over 95 % epileptic components are retained, which demonstrates that the proposed method is an efficient tool in removing artifacts from epileptic EEGs.

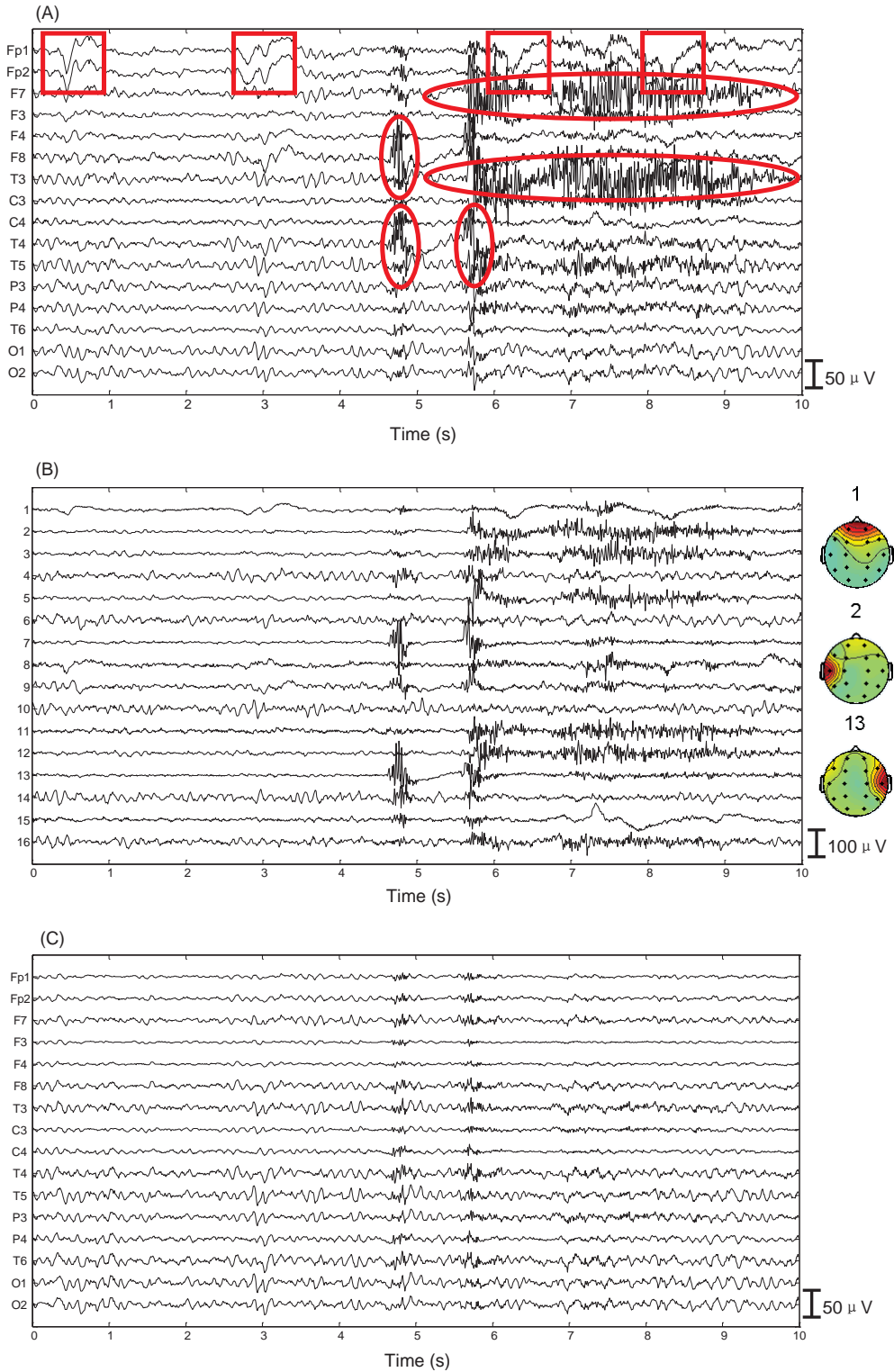


Fig. 4. Performance of the algorithm on interictal EEG



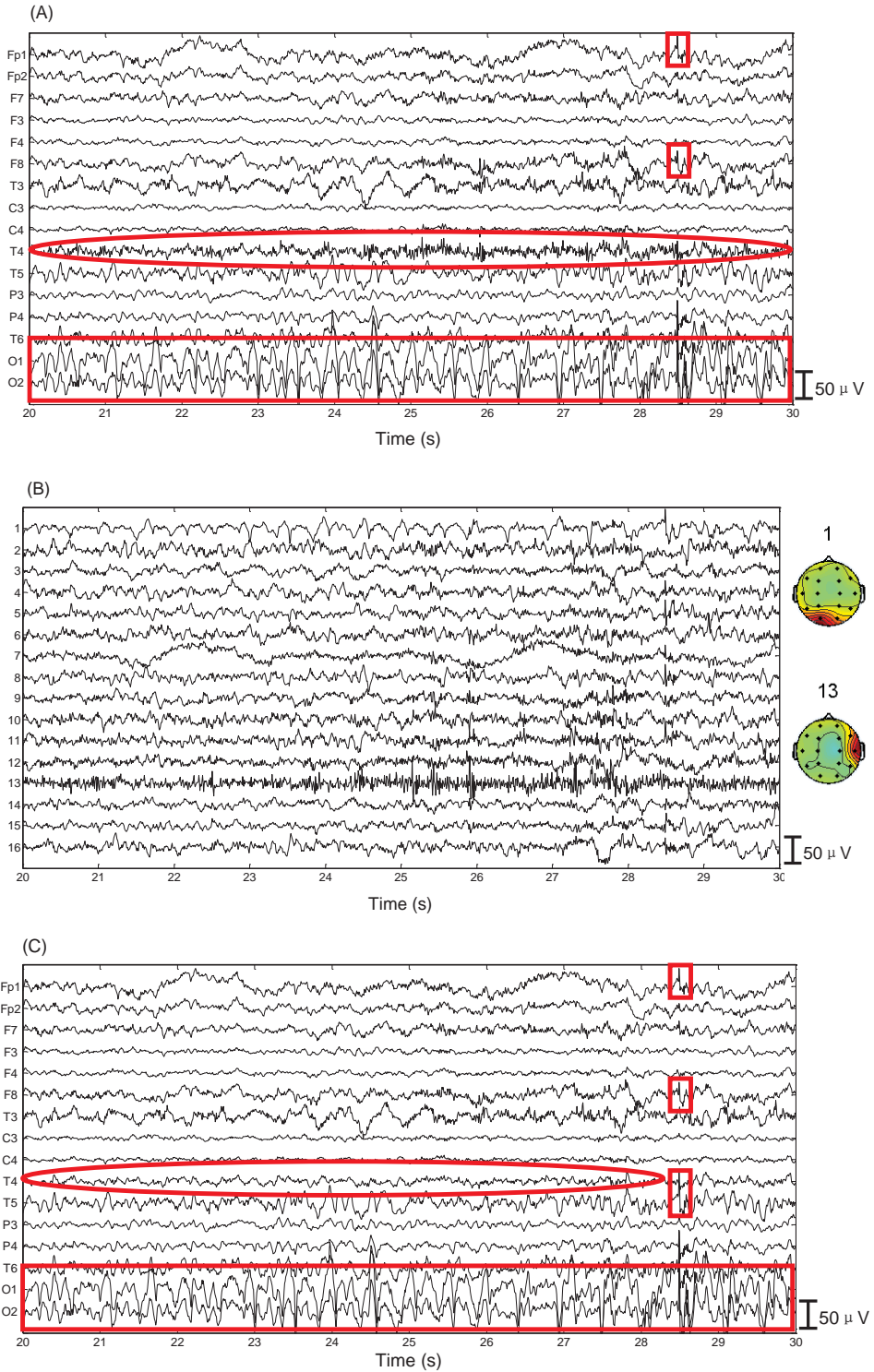


Fig. 5. Performance of the algorithm on ictal EEG

## 4. Discussion and conclusion

### 4.1. Discussion

A very important issue is the partition of independent components. In the proposed method feature vectors are calculated based on the partitioned epochs of independent components (30 s). This is very important because some independent components are a mixture of EEG and artifacts. Extracting the features using the entire independent component may obscure the artifact segments. On the other hand, the length of partitioned epoch is a key issue. If the partitioned epoch is too short, the computational load will increase substantially. Meanwhile this will also lead to the high probability of partitioning low-frequency artifacts into different epochs, which obscures the artifact features and eventually affects the classification accuracy [8]. After exploring the common artifacts in EEG, we decide that 5 s epoch is enough to describe the characteristics of the artifacts.

### 4.2. Conclusion

In this paper we have presented a robust method for removing artifacts from epileptic EEG based on ICA and SVM. ICA is used to decompose the acquired EEG data into independent components. Each independent component is then partitioned into 5 s epochs. With the predefined eight features in time and frequency domain, including Hurst exponent, skewness, kurtosis, largest Lyapunov exponent and frequency-band energy, the artifact epochs can be automatically identified with the trained support vector machine. The sum of epochs representing artifacts is then used to determine whether to reject or preserve each independent component. Artifact-free EEGs are reconstructed with the remaining independent components. Results show that the proposed algorithm can identify and remove a variety of artifacts in interictal and ictal EEGs, such as baseline drift, ECG, EMG, EOG and power frequency interference. Compared with traditional automatic artifact removal methods [7, 20], the proposed algorithm in this paper does not require reference channels (e.g. ECG, EOG), which would be more appropriate for clinical EEG data.

**Table 1.** Performance of the algorithm on the validation set

Number	Independent components	Artifact components	EEG components	Epileptic EEG components	Global classification error	Classification error of epileptic EEG components
1	320	145	175	28	9.38 %	0 %
2	320	185	135	26	8.44 %	3.85 %
3	320	99	221	87	6.25 %	11.49 %
4	320	213	107	30	12.50 %	3.33 %
5	320	126	194	85	11.56 %	5.88 %
6	320	160	160	62	15.31 %	3.23 %
7	320	143	177	39	12.81 %	7.69 %
8	320	138	182	69	9.38 %	5.80 %
9	320	111	209	23	10.31 %	0 %
10	320	192	128	28	8.75 %	0 %
11	320	73	247	77	10.63 %	7.79 %
12	320	155	165	52	16.56 %	3.85 %
13	320	142	178	15	13.44 %	6.67 %
14	320	159	161	35	7.50 %	5.71 %
15	320	163	157	27	5.31 %	3.70 %
Total	4800	2204	2596	683	10.54 %	4.60 %

## Acknowledgements

This work was supported by the National Natural Science Foundation of P. R. China (Approval No. 51005176) and Doctoral Fund of Ministry of Education of China (Approval No. 20100201120003).

## References

- [1] **Z. Vasickova, M. Augustynek** New method for detection of epileptic seizure. *Journal of Vibroengineering*, Vol. 11, Issue 2, 2009, p. 279-282.
- [2] **N. Agata, K. Andrzej, N. Marcin** Biomedical signal identification and analysis. *Journal of Vibroengineering*, Vol. 14, Issue 2, 2012, p. 546-552.
- [3] **E. Kaniusas, A. Podlipkyte, A. Alonderis** Relation in-between autonomic cardiovascular control and central nervous system activity during sleep using spectrum-weighted frequencies. *Journal of Vibroengineering*, Vol. 12, Issue 1, 2010, p. 106-112.
- [4] **N. Y. Bian, B. Wang, Y. Cao, L. M. Zhang** Automatic removal of artifacts from EEG data using ICA and exponential analysis. *Lecture Notes in Computer Science*, Vol. 3972, 2006, p. 719-726.
- [5] **S. Boudet, L. Peyrodie, P. Galois, C. Vasseur** Filtering by optimal projection and application to automatic artifact removal from EEG. *Signal Process.*, Vol. 87, Issue 8, 2007, p. 1978-1992.
- [6] **C. James, O. Gibson** Temporally constrained ICA: an application to artifact rejection in electromagnetic brain signal analysis. *IEEE Transactions on Biomedical Engineering*, Vol. 50, Issue 9, 2003, p. 1108-1116.
- [7] **C. A. Joyce, I. F. Gorodnitsky, M. Kutas** Automatic removal of eye movement and blink artifacts from EEG data using blind component separation. *Psychophysiology*, Vol. 41, Issue 2, 2004, p. 313-325.
- [8] **P. Le Van, E. Urrestarazu, J. Gotman** A system for automatic artifact removal in ictal scalp EEG based on independent component analysis and Bayesian classification. *Clinical Neurophysiology*, Vol. 117, Issue 4, 2006, p. 912-927.
- [9] **S. Vorobyov, A. Cichocki** Blind noise reduction for multisensory signals using ICA and subspace filtering, with application to EEG analysis. *Biological Cybernetics*, Vol. 86, Issue 4, 2002, p. 293-303.
- [10] **C. Justten, J. Herault** Blind separation of sources, Part I: An adaptive algorithm based on neuromimetic architecture. *Signal Process.*, Vol. 24, Issue 1, 1991, p. 1-10.
- [11] **P. Comon** Independent analysis – a new concept? *Signal Process.*, Vol. 36, Issue 3, 1994, p. 287-314.
- [12] **A. Hyvarinen, E. Oja** A fast fixed-point algorithm for independent component analysis. *Neural Computing*, Vol. 9, Issue 7, 1997, p. 1483-1492.
- [13] **A. Delorme, S. Makeig, T. Sejnowski** EEGLAB: an open source toolbox for analysis of single-trial EEG dynamics including independent component analysis. *Journal of Neuroscience Methods*, Vol. 134, Issue 1, 2004, p. 9-21.
- [14] **M. De Vos, W. Deburchgraeve, P. J. Cherian, V. Matic, R. M. Swarte, P. Govaert, et al.** Automated artifact removal as preprocessing refines neonatal seizure detection. *Clinical Neurophysiology*, Vol. 122, Issue 12, 2011, p. 2345-2354.
- [15] **H. E. Hurst, R. P. Black, Y. M. Simaikda** Long Term Storage: an Experimental Study. Constable, London, 1965.
- [16] **S. Leor, S. Saeid, C. Jonathon** Artifact removal from electroencephalograms using a hybrid BSS-SVM algorithm. *IEEE Signal Process. Letter.*, Vol. 12, Issue 10, 2005, p. 721-724.
- [17] **A. Das, P. Das, A. B. Roy** Applicability of Lyapunov exponent in EEG data analysis. *Complex International*, Vol. 9, Issue 1, 2002, p. 1-8.
- [18] **H. Adeli, Z. Zhou, N. Dadmehr** Analysis of EEG records in an epileptic patient using wavelet transform. *Journal Neuroscience Methods*, Vol. 123, Issue 1, 2003, p. 69-87.
- [19] **T. Wu, G. Z. Yan, B. H. Yang, H. Sun** EEG feature extraction based on wavelet packet decomposition for brain computer interface. *Measurement*, Vol. 41, Issue 6, 2008, p. 618-625.
- [20] **D. Talsma** Auto-adaptive average: detecting artifacts in event-related potential data using a fully automated procedure. *Psychophysiology*, Vol. 45, Issue 2, 2008, p. 216-228.